Cleaner Engineering and Technology 19 (2024) 100731

Contents lists available at ScienceDirect

Cleaner Engineering and Technology

journal homepage: www.sciencedirect.com/journal/cleaner-engineering-and-technology

# An experimental assessment of simultaneous reduction in vehicle tailpipe emissions employing desirability function analysis

Amanuel Gebisa [a,*], Girma Gebresenbet [b], Rajendiran Gopal [c], Ramesh Babu Nallamothu [a]

[a] Mechanical Engineering Department, Adama Science and Technology University, Adama, P.O. Box 1888, Ethiopia
[b] Division of Automation and Logistics, Department of Energy and Technology, Swedish University of Agricultural Science, P.O. Box 7032, 750 07, Uppsala, Sweden
[c] Automotive Engineering Program, Department of Mechanical and Industrial Engineering, Bahir Dar Institute of Technology, Bahir Dar University, P.O.Box 79, Ethiopia

ARTICLE INFO

*Keywords:*
Desirability function analysis
Road slope
Tailpipe emissions

ABSTRACT

In vehicles powered by fuel, the effort to minimize CO and HC emissions through various strategies leads to an increase in $CO_2$, contributing to global warming. This study aimed to experimentally assess the simultaneous reduction of vehicle tailpipe emissions of CO, HC, and $CO_2$ using desirability function analysis (DFA). On predetermined routes in Addis Ababa city, two vehicles were tested for on-road emissions at five various speeds and on five various road slopes using a portable emissions tester. Surface plots were used to display how the tailpipe emissions of $CO_2$, CO, and HC vary with changes in vehicle speed and road gradient. The DFA results revealed that the optimal speed for simultaneous reduction of CO, HC, and $CO_2$ emissions was 40 km/h on a flat route and 30 km/h on a 2-degree uphill, with composite desirability of 0.83 and 0.72, respectively. This study found that a speed of 30 km/h on a flat road increased $CO_2$ by 2.82%, CO by 18.97%, and HC by 5.28% compared to an optimized vehicle speed of 40 km/h. On a 2-degree gradient, a vehicle traveling at 20 km/h exhibited a 4% increase in $CO_2$ emissions, a 23.92% increase in CO emissions, and a 1.26% decrease in HC emissions compared to the optimized speed of 30 km/h. Adjusting speed limits according to road gradients is recommended to minimize vehicle tailpipe emissions simultaneously using DFA. This approach contributes to lowering air pollution by reducing pollutant emissions from vehicles through optimized speeds.

## 1. Introduction

The use of petrol and diesel fuels makes vehicles major contributors to air pollution in urban areas (Alhassan Sati and Johnson Dare, 2022). Numerous variables affecting the fuel consumption and exhaust emission rate, which make the emission estimation more complex (Śarkan et al., 2022). Cities are experiencing greater traffic congestion as a result of increased vehicle and population densities negatively impacting environment, social, and economic conditions (Shepelev et al., 2023). Several factors impact vehicle emissions and fuel consumption, including vehicle design, and performance, the local weather condition, road gradient, and operating circumstances (Liu et al., 2019). A positive road gradient leads to an elevated in vehicle-specific power (VSP) at a given speed, resulting in higher average emission outputs (Meng et al., 2023).

European standards are established through a set of regulations that implement progressively stricter limits (Donateo and Filomena, 2020). Real-time monitoring of emissions provides comprehensive data that can be employed to identify real-world estimations at micro-scale events, significantly influencing overall emissions, as opposed to the chassis dynamometer testing method (Meena and Singh, 2022). Presently, the primary focus of the majority of researchers lies in on-road vehicular emission measurement in real-time.

Conducting on-road emissions tests enables the assessment of the vehicle's pollutant emissions and facilitates informed decision to reduce $CO_2$ emissions related to vehicles. The on-road test results from the study conducted by (Karimipour et al., 2021) indicated that opting for the optimized route instead of the standard one has the potential to cut down fuel consumption and GHG emissions by 62% for heavy vehicles. In (Sher et al., 2021) study on hybrid electric vehicles, the powertrain's operating efficiency was optimized using various algorithms to maximize fuel efficiency and minimize exhaust emissions. The proposed method indicates potential reductions of 5% in fuel consumption, 50% in CO emissions, and an improvement of 15% in engine efficiency. There are various advantages to decreasing $CO_2$ emissions from vehicles. Enhancing the fuel efficiency of vehicles not only serves on fuel expenses

* Corresponding author.
*E-mail address:* amanuel.gebisa@astu.edu.et (A. Gebisa).

https://doi.org/10.1016/j.clet.2024.100731
Received 29 September 2023; Received in revised form 24 January 2024; Accepted 1 February 2024
Available online 12 February 2024

reduction but also mitigates the impacts of climate change, fosters a healthier environment, and contributes to overall well-being. Implementing measures to reduce $CO_2$ emissions is crucial for promoting healthier lives for both present and future generation.

A thorough analysis of the literature on vehicle emissions has been carried out. The limited number of previous studies that is relevant to this study, which focused on the assessment of on-road vehicle tailpipe emissions, were reviewed below. The analysis by (Meng et al., 2023) revealed that the average emissions rates were sensitive to variations in VSP and road slope. Recently, (Cvitanić et al., 2023) looked at how a vehicle's fuel consumption and emissions are affected by road alignment, while (Posada-Henao et al., 2023) examined the effects of vehicle weight and road gradient on truck fuel consumption.

According to the findings of (Meng et al., 2023), roads with grades higher than 3% produce three to six times as much emissions as those with grades lower than −3%. According to a study by (Liu et al., 2019), fuel consumption rate was underestimated by 12% when road grade was ignored at 2%. (Costagliola et al., 2018) discovered that a road with a 5% slope produces over a 100% increase in $CO_2$ when compared to a flat road. On the other hand, a road slope of −4% reduces $CO_2$ emissions by over 70%, when compared to level roads. Consequently, the road gradient and its impact on emissions must be taken into account while designing roadways. The environmental effects of varying road gradients should also be taken into account while choosing the most efficient path of travel. Road grades between 0 and 5% raised $CO_2$ by 65–81% (Gallus et al., 2017). According to a study by (Triantafyllopoulos et al., 2019), driving uphill while using dynamic driving increases $CO_2$ emissions three times. Referring to (Pavlovic et al., 2020), the study demonstrated that as road gradient increases, so does the fuel consumption discrepancy. Furthermore, (Salihu et al., 2023), discovered that emissions of CO, HC, and $NO_X$ are more susceptible to increases on upward slopes than on downward slopes.

As per these studies, driving on a road that has a positive slope can significantly increase vehicle emissions and fuel usage. To the best of the authors' knowledge, studies has been conducted on vehicle on-road emissions; however, the optimal point at which $CO_2$, HC, and CO emissions can simultaneously minimized has not been assessed. The driving dynamics need to be appropriately optimized in order to lower fuel consumption and emissions. This study utilized desirability function analysis (DFA) to ascertain the optimal driving speed for the selected road slope to reduce $CO_2$, HC, and CO emissions simultaneously.

The DFA, recognized as a widely employed optimization technique, assigns values to a set of responses and identifies the variables that optimize these response values (Ali et al., 2022). For the concurrent optimization of multiple responses, both academia and industry frequently employ the desirability function analysis method (Thorisingam and Mustafa, 2022). In recent studies, (Ali et al., 2022) utilized DFA to identify the risk factors associated with the lowest CO2 emissions in Africa, while (Perec, 2022) applied DFA to optimize machining settings for high-pressure abrasive water jet cutting of Hardox 500 steel. DFA was used for this study because it can comprehensively assess multiple response variables at the same time and coherently express each variable's desirability. Moreover, DFA stands out due to its thorough evaluation of several responses, customization through weighting, and user-friendly interpretation, making it a reliable and useful optimization option for this study.

In the context of IC engines, employing various strategies to minimize the emission of pollutant gases like CO and HC inadvertently leads to an increase in $CO_2$ levels. This elevation contributes negatively to global warming through the greenhouse effect. Mitigating CO, HC, and $CO_2$ simultaneously poses a significant challenge. To address this, a comprehensive analysis, including a full factorial examination, was conducted. Utilizing DFA, we identified the optimal driving range for urban routes, effectively reducing CO, HC, and $CO_2$ emissions concurrently. The results obtained demonstrated that the identified optimal driving range for urban routes successfully achieved a simultaneous reduction in CO, HC, and $CO_2$ emissions. This approach offers an applicable method for curbing emissions from IC engines, applicable for developing emission reduction plans across various engine types and vehicles. Moreover, it serves as a valuable reference for future research endeavours aimed at lowering emissions within the transportation sector.

## 2. Materials and methods

This investigation utilized GPS, portable emissions testers, and petrol- and diesel-powered vehicles to collect data. The study employed an experimental approach involving the selection of vehicles, route determination, emission measurements, and the application of full factorial and desirability analysis for data analysis. A portable emissions tester, installed on the selected vehicles, was employed to measure tailpipe emissions released into the atmosphere while the vehicles were traveling on-road. The flow chart of this study is presented in Fig. 1.

### 2.1. Study area

On-road data collection took place in Addis Ababa, Ethiopia, utilizing different road slope sections as outlined in the experimental design. Fig. 2 (a – d) depicts four route chosen as study sites in Addis Ababa, Ethiopia. These selected routes experienced significant traffic, with high pollution often occurring during peak hours, primarily due to traffic congestion. This exhibited in a decline in air quality, contributing to a various health issues for residents and workers in the vicinity.

### 2.2. Design of the experiment

In the experimental design of this study, a full factorial design was employed as a method to assess how different levels of inputs impact outputs through the careful designing and executing of the experiment. This approach allows for the testing of all input combinations while thoroughly controlling for other variables. It enables the identification of the optimal input/output combination for achieving the most effective output. In this study, two factors with five levels were utilized, as illustrated in Table 1. The factors consisted of vehicle speed and road slope, with three replications at constant vehicle weight. The number of vehicles used in data collection was two, with mileages of 71,446 km and 90,277 km for the petrol and diesel vehicles, respectively. The petrol vehicle used in data collection is 7 years old, while the diesel vehicle is 5 years old. In the city of AA, the selection of road slope and vehicle speed levels for this study took into consideration the road slope and vehicle speed limit. The levels of each factor were deliberately changed to assess their influence on tailpipe emissions, encompassing $CO_2$, CO, and HC. The standard order presented in Table 1 refers to a predefined sequence that serves as a reference in the experimental process, while run order refers the actual sequence of experimental trials followed in this study.

### 2.3. Data collection

In this study, we employed a portable emissions tester, the GA5000 model manufactured by GeoTech, to measure tailpipe emissions from selected vehicles. The number of vehicles used for data collection was two, one powered by petrol and the other by diesel. Throughout the entire data collection process, each vehicle was loaded with four passengers (275 kg). Fig. 3 depicts a central unit featuring integrated sensors and a system designed for real-time data acquisition, processing, recording, and display. The gas analyser utilized measured the concentrations of CO, $CO_2$, $O_2$, HC, and $H_2S$; with detailed specifications outlined in Table 2 for the portable emission tester. However, for this study purposes, we employed the GA5000 to measure only $CO_2$, CO, and HC emissions. Sampling of tailpipe emissions was conducted using 3 mm outer diameter stainless steel probes equipped with clamps. An 8 m tube connected the probe to the portable emissions tester located inside the

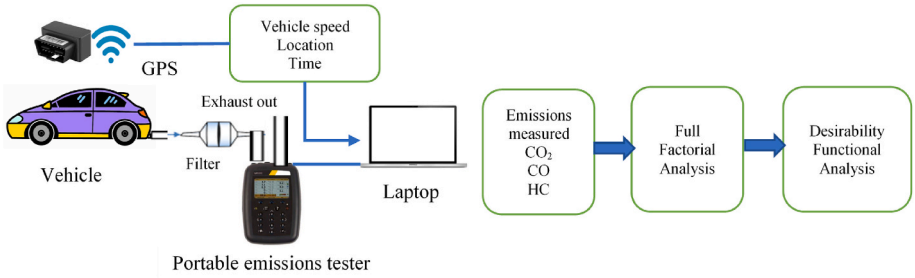


**Fig. 1.** Overall study flow chart.


**Fig. 2.** Selected routes for data collection.

**Table 1**
Full factorial experimental design.

| Standard order | Run order | Vehicle speed (km/h) | Road slope (degree) | Standard order | Run order | Vehicle speed (km/h) | Road slope (degree) |
|---|---|---|---|---|---|---|---|
| 10 | 1 | 20 | 6 | 17 | 14 | 40 | 0 |
| 24 | 2 | 50 | 4 | 18 | 15 | 40 | 2 |
| 11 | 3 | 30 | −2 | 25 | 16 | 50 | 6 |
| 1 | 4 | 10 | −2 | 12 | 17 | 30 | 0 |
| 22 | 5 | 50 | 0 | 9 | 18 | 20 | 4 |
| 13 | 6 | 30 | 2 | 15 | 19 | 30 | 6 |
| 21 | 7 | 50 | −2 | 7 | 20 | 20 | 0 |
| 5 | 8 | 10 | 6 | 3 | 21 | 10 | 2 |
| 20 | 9 | 40 | 6 | 8 | 22 | 20 | 2 |
| 14 | 10 | 30 | 4 | 23 | 23 | 50 | 2 |
| 2 | 11 | 10 | 0 | 19 | 24 | 40 | 4 |
| 16 | 12 | 40 | −2 | 6 | 25 | 20 | −2 |
| 4 | 13 | 10 | 4 | | | | |

vehicle. In this study, we assumed that the fractional volume of a specific gas entering the data collection probe of the tester is equal to the fraction of that particular gas considered out of the total volume. The experiment adhered to the procedures outlined in Fig. 4.

At the beginning of each test, the portable gas analyser was positioned on the rear passenger seat, powered on and allowed to warm up for 10 min. It operated on an internal battery, which could be recharged using a 220 V alternative current power supply. When fully charged, the

a) Exhaust sampling line b) Measuring device during the experiment

**Fig. 3.** The portable gas tester utilized during the on-road emissions test.

**Table 2**
Technical specifications of portable emission tester employed in this study.

| Tailpipe emissions | Measurement type | Unit | Measurement uncertainty |
|---|---|---|---|
| $CO_2$ | By dual wavelength infrared sensor with reference channel | % | ±0.5% (vol) |
| CO | Internal electrochemical sensor | % | ±2% (vol) |
| HC | Internal electrochemical sensor | % | ±2% (vol) |

battery could provide the portable emissions analyser for 8 continuous hours. Additionally, GPS was utilized to gather data on the vehicle's speed and location. The portable gas analyser captured and stored the raw data internally. Following the installation of its data logging software, the data was transferred to the laptop via a USB cable. The GPS data collected was accessed through a web-based portal. Subsequently, the collected emissions data was correlated with vehicle speed and location data. Finally, the experimental data was organized and saved as an Excel file for further processing in Minitab 21.

The choice of older vehicles allowed for robust measurements with a portable emissions analyser without concerning emissions standards. Table 3 provides details about both vehicles. Both vehicles were fuelled with commercially available fuel obtained from local fuel stations. Experiments were carried out between June 7$^{th}$ and June 11$^{th}$, 2023, with ambient temperatures ranging from 12 °C to 25 °C.

### 2.4. Data analysis

#### 2.4.1. Full factorial analysis (FFA)

The portable gas tester used in this study captured the raw emissions data for $CO_2$, HC, and CO. To determine the emissions in grams per kilometre, the tailpipe emissions in percentage were converted to g/km using the correlation adopted by (Pilusa et al., 2012). The procedures for unit conversion of CO, $CO_2$, and HC emissions are outlined in equations (1)–(3).

$$CO_2\left(g/_{km}\right) = 166.3 \times CO_2\ (\%vol) \tag{1}$$

$$CO\left(g/_{km}\right) = 9.66 \times 10^{-3} \times CO\ (\%vol) \tag{2}$$

**Table 3**
Specifications of vehicles used in this study.

| Parameters | Petrol vehicle | Diesel vehicle |
|---|---|---|
| Vehicle manufacturer | Sokon Group | Toyota |
| Vehicle model | DFSK Glory | Land cruiser |
| Model year | 2016 | 2019 |
| Engine capacity (litre) | 1.3 | 4.16 |
| Maximum power output | 112 kW | 96 kW @3800 rpm |
| Gross vehicle weight (kg) | 2035 | 2720 |
| Gearbox | Manual | Manual |
| Accumulated mileage (km) | 71,446 | 90,277 |
| Fuel control strategy | Electronic fuel injection | Conventional type |
| Emission control | NA | NA |

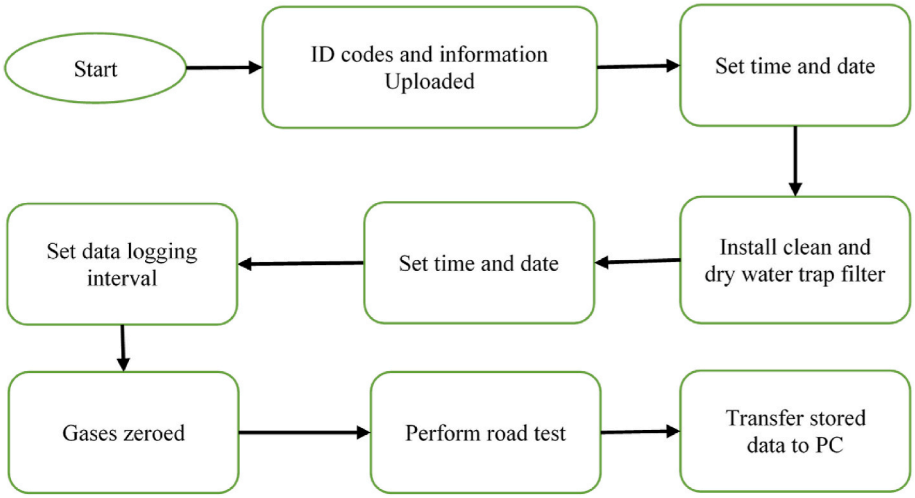


**Fig. 4.** Procedures of experimental data collection.

$$HC\left(g/km\right) = 5.71 \times 10^{-3} \times HC\ (\%vol) \quad (3)$$

After converting the emissions unit to g/km, we employed a FFA. This analysis encompassed the main effect analysis, regression analysis and surface plot. This allows us to identify the most significant variables influencing the levels of emissions and their interactions. Moreover, it enables to assess the accuracy of the model.

Employing the conventional regression method, we developed predictive models to understand the connection between input factors and output responses of a system. In this study, regression analysis was used to model and evaluate the relationship between factors such as vehicle speed and road slope and their corresponding performance attributes, such as $CO_2$, CO, and HC. Equation (4) demonstrates a general linear regression model incorporating multiple predictors.

$$Y = c + c_1\chi_1 + c_2\chi_2 + \ldots + c_{12}\chi_1\chi_2 + c_{13}\chi_1\chi_3 + \ldots + c_{11}\chi_1^2 + c_{22}\chi_2^2 + \ldots (4)$$

Where: Y is the response, $\chi_1$, $\chi_2$, $\chi_3$ … are the independent factors, $c_1$, $c_2$, $c_{12}$, $c_{22}$ … are the cofficients of regression.

#### 2.4.2. Desirability function analysis (DFA)

This study reduced $CO_2$, CO, and HC emissions simultaneously employing DFA. The objective of the optimization process is to minimize, maximize, or attain a target value for the responses, donated as $y_i$, utilizing the desirability function $d_i$ ($y_i$). Each $y_i$ value is assigned a score ranging from 0 to 1, where 1 represents the most desirable value and 0 indicates the least desirable value (Devarajaiah and Muthumari, 2018).

DFA depends on a function known as composite desirability to consolidate multiple response characteristics into a unified response function (Perec, 2022). The analysis was carried out through the following steps to obtain the solution.

1. Calculate desirability index:

Since the primary goal of this study is to minimize $CO_2$, CO, and HC, the preference is for the smallest achievable value. Consequently, the findings of this study can be utilized to pinpoint the most effective operating range for emissions reduction. When the output response reaches the minimum possible value, the $d_i$ factor is computed as follows (Ali et al., 2022):

$$d_i = \begin{cases} 1, y_i \le y_{min} \\ \left(\dfrac{y_i - y_{max}}{y_{min} - y_{max}}\right)^r, y_{min} \le y_i \le y_{max}, r \ge 0 \\ 0, y_i \ge y_{min} \end{cases} \quad (5)$$

where: $d_i$ is the individual desirability, $y_i$ is the expected value, $y_{min}$ is the lower tolerance limit, $y_{max}$ is the upper tolerance limit, and r is the weight.

2. Calculate composite desirability

The individual desirability indices for all responses were combined to a single value using equation (5) to generate the overall desirability function (D).

$$D = \sqrt[w]{d_1^{w1} \times d_2^{w2} \ldots d_i^{wi}} \quad (6)$$

where: D is the overall desirability, $d_i$ is individual desirability, $w_i$ is the weight of the response $y_i$, and w is the sum of the individual weights.

Finally, determine the optimum combination of level control settings. The high composite desirability value suggests a low emissions level.

## 3. Results and discussion

### 3.1. General factorial regression for $CO_2$

Figs. 5 and 6 illustrate the main effect plot of $CO_2$ emissions for petrol and diesel vehicles, respectively, under different road grades. General, the average $CO_2$ emissions shows a noticeably increased with road gradient. Specifically, for petrol vehicles, the $CO_2$ emissions rates at road gradients of 2°, 4°, and 6° were 16.25%, 28.58%, and 43.36% higher, respectively, compared to the emission rates on flat road. In contrast, for diesel vehicles, the $CO_2$ emissions rate at road gradients of 2°, 4°, and 6° were 53.7%, 91.08%, and 245.85% higher, respectively, than the emission rates on level roads, with a 36% reduction observed in $CO_2$ during a downhill slope of −2°. These variations are attributed to the strong correlation between the $CO_2$ emissions rate and fuel consumption (Meng et al., 2023).

On roads with positive road gradients, vehicles demand more power, leading to increased fuel consumption and $CO_2$. The $CO_2$ of an engine are affected by the oxygen content in the combustion chamber and its temperature (Wang et al., 2022). In this study, petrol vehicles emit 45.78%, 46.42%, 48.68%, 42.02%, and 42.45% more $CO_2$ emissions than diesel vehicles at 10, 20, 30, 40, and 50 km/h, respectively. With respect to road gradients, petrol vehicles emit 68%, 57%, 45%, 37.97%, and 28.8% more $CO_2$ emissions than diesel vehicles at −2, 0, 2, 4, and 6° road gradients, respectively.

At a 95% confidence level, regression analysis was conducted using Minitab 21. Equations (7) and (8) were derived from the regression analysis equation (4), to evaluate the relationship between vehicle speed and road slope variables and the performance attributes of $CO_2$ emission. Equation (7) represents the regression equation for $CO_2$ emissions of the petrol vehicle, while equation (8) presents the regression equation for $CO_2$ emissions of the diesel vehicle.

$$CO_2(g/km) = 189.77 + 0.682 \times V + 16.89 \times S - 0.0615 \times V \times S \quad (7)$$

$$CO_2(g/km) = 79.1 + 0.461 \times V + 17.82 \times S - 0.0571 \times V \times S \quad (8)$$

where V is vehicle velocity in km/h, and S is road slope in degree.

The extent to which the regression model contributes to explaining is donated by the R-square. R-square values close to 1 suggests that the regression model effectively accounts for a significant portion of the dependent variables. The values of R-square and adjusted R-square are shown in Table 4, indicating that the accuracy of the model results were optimal for both petrol and diesel vehicles. These findings imply that the regression models formulated for petrol and diesel vehicles serve as dependable approaches for determining $CO_2$.

Surface plots generated by the Minitab 21 are employed to examine the variations of $CO_2$ with road slope and vehicle speed, as depicted in Figs. 7 and 8 for petrol and diesel vehicles, respectively.

### 3.2. General factorial regression for CO

The main interaction effects of CO emissions rates for various road slopes in petrol and diesel vehicles are illustrated in Figs. 9 and 10, respectively. Generally, the average CO emissions rate exhibits a noticeable increase with an elevation in road slope and decreases with an increase in vehicle speed. Specifically, for petrol vehicles, the CO emissions on roads with slopes of 2°, 4°, and 6° were 37.76%, 168.47%, and 177.1% higher, respectively, than the rates a level roads, with a reduction of 10.27% observed during downhill driving at a −2°. On the other hand, for diesel vehicles, the CO emissions on roads with slopes of 2°, 4°, and 6° were 42.84%, 76.48%, and 104% higher, respectively, than the rates on level road, and an 8.9% reduction in CO was observed on downhill roads with −2° slope. The findings of this study indicated that diesel vehicles emit 11.04%, 11.36%, 2.38%, 9.69% and 8.77% less CO emissions than petrol vehicles at speeds of 10, 20, 30, 40, and 50 km/

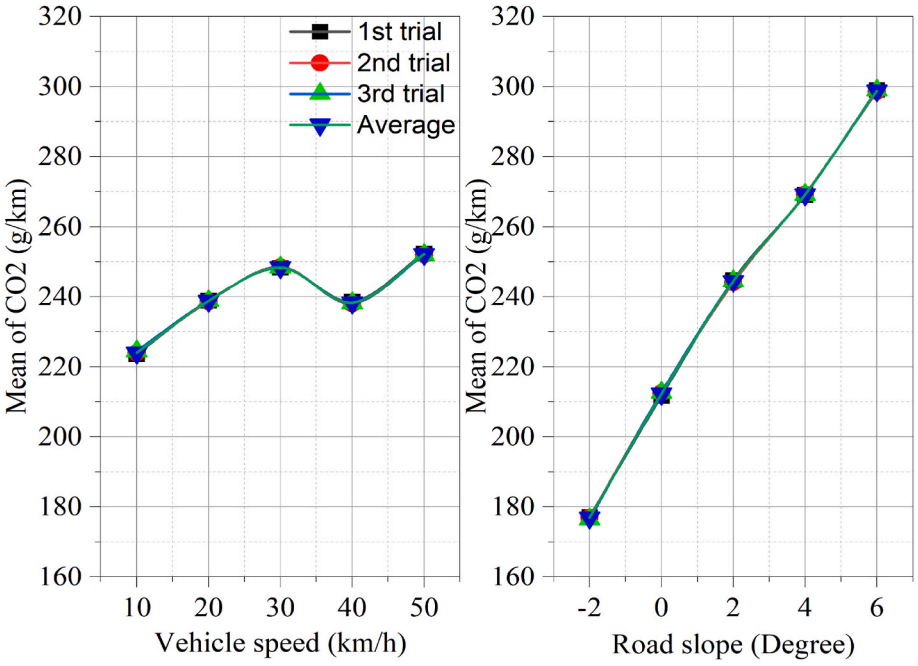


**Fig. 5.** $CO_2$ main effect plot for petrol vehicle.

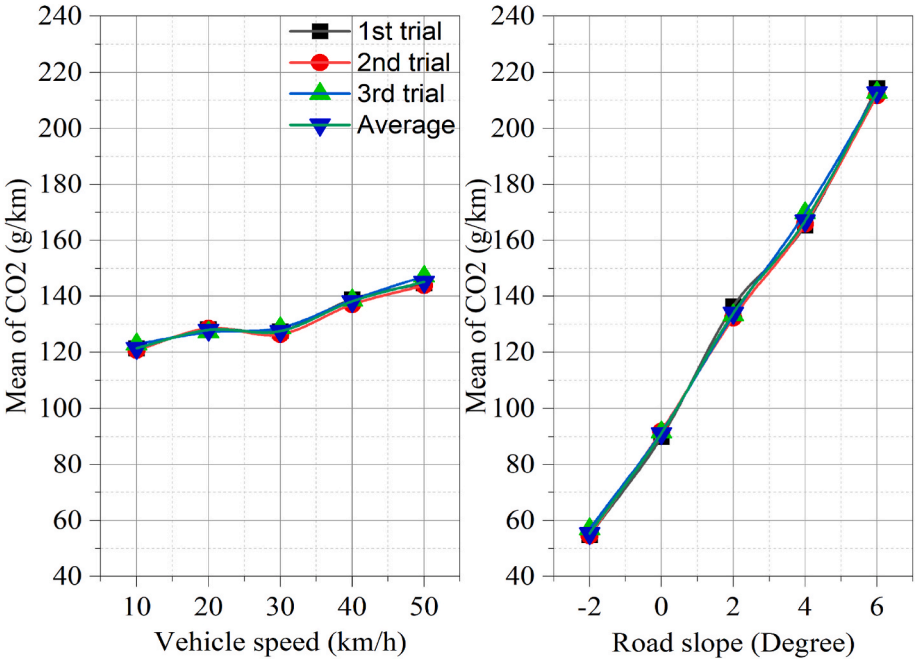


**Fig. 6.** $CO_2$ main effect plot for diesel vehicle.

**Table 4**
Model summary for $CO_2$.

| Vehicle type | R-square (%) | R-square (adj) (%) | R-square (pred) (%) |
|---|---|---|---|
| Petrol | 99.98 | 99.97 | 99.96 |
| Diesel | 96.03 | 95.47 | 94.48 |

h, respectively. Additionally, the CO emissions from petrol vehicles at −2, 0, 2, 4, and 6° road gradients are 12.5%, 13.32%, 10.57%, 9.94%, and 3.62% higher than those from diesel vehicles.

The fitted regression models for CO emissions from petrol-powered and diesel-powered vehicles are presented in equations (9) and (10), respectively. Both regression models for petrol and diesel vehicles exhibited the highest levels of accuracy and precision in the findings, as indicated by the value of R-square and adjusted R-square in Table 5.

$$CO\ (g/km) = 77.83 + 1.224 \times V + 5.49 \times S - 0.0453 \times V \times S \quad (9)$$

$$CO\ (g/km) = 68.48 + 1.075 \times V + 5.38 \times S - 0.0367 \times V \times S \quad (10)$$

where V is vehicle velocity in km/h, and S is road slope in degree.

Furthermore, the surface plots generated, as shown in Figs. 11 and 12, illustrate the variations of CO with vehicle speed and road gradient for petrol and diesel vehicles, respectively. In consideration of this, it can

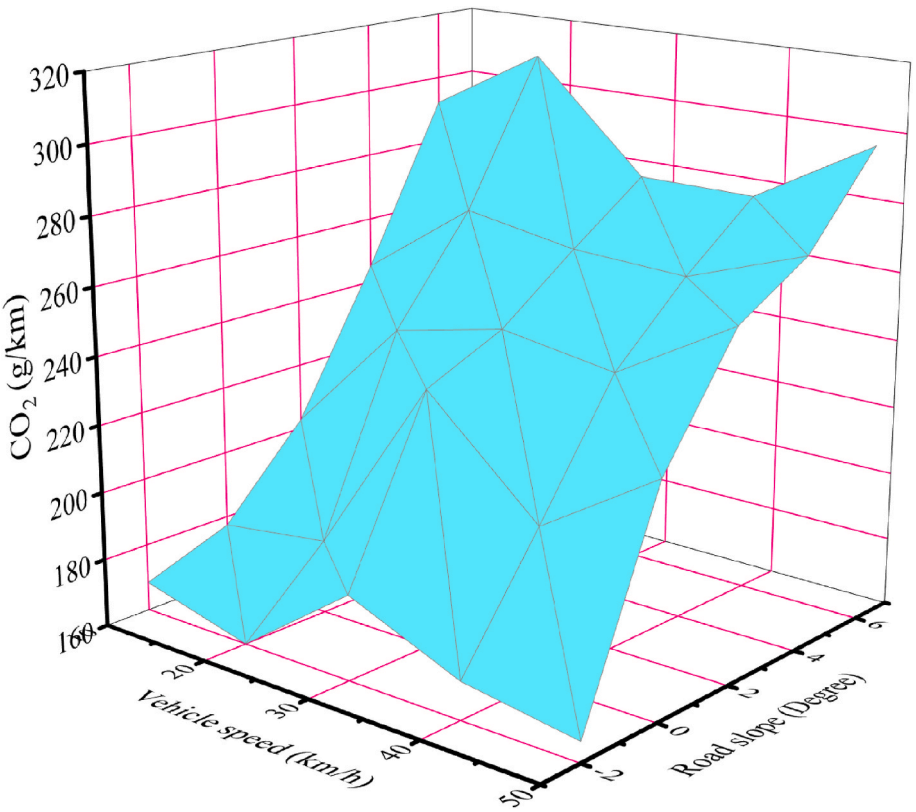


**Fig. 7.** Surface plot of $CO_2$ emissions for petrol vehicles.

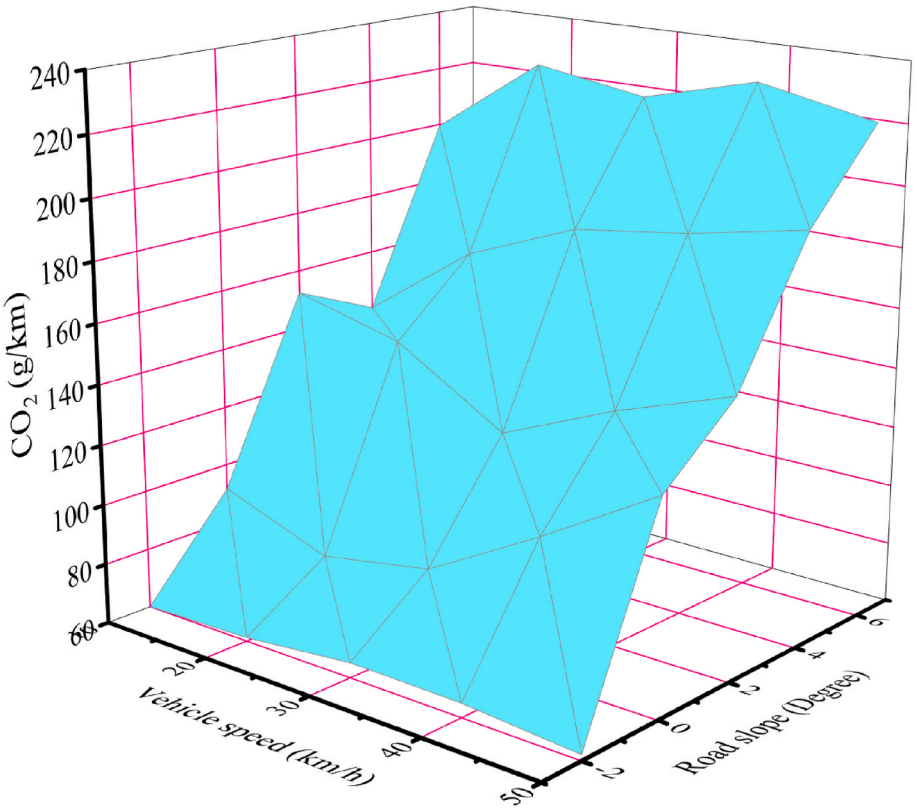


**Fig. 8.** Surface plot of $CO_2$ emissions for diesel vehicles.

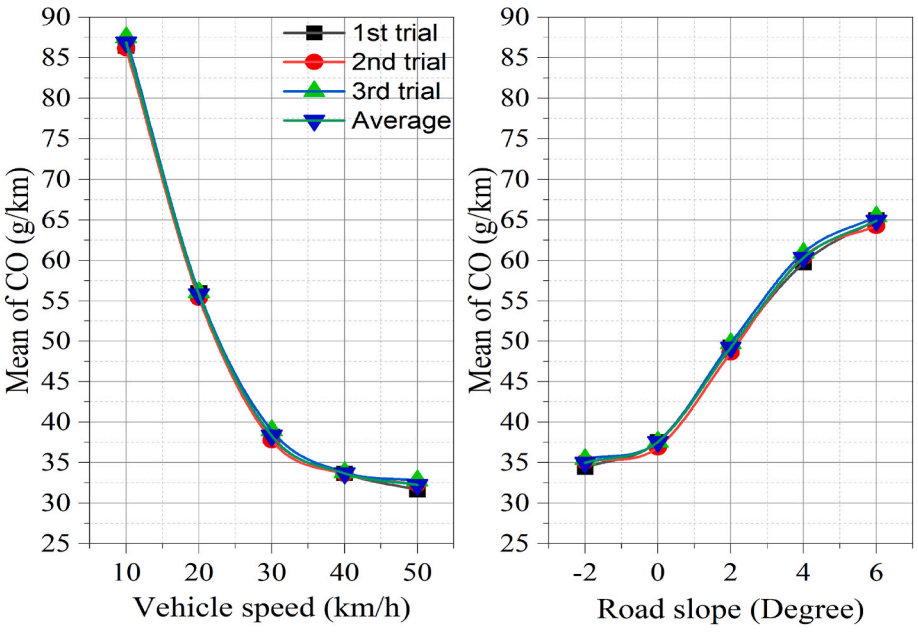


**Fig. 9.** CO main effect plot for petrol vehicle.

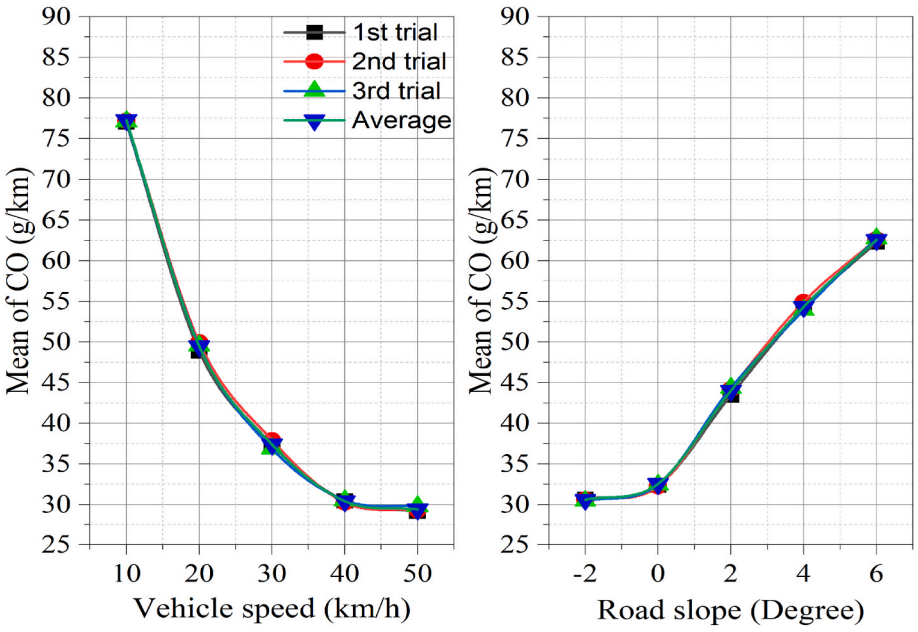


**Fig. 10.** CO main effect plot for diesel vehicle.

**Table 5**
Model summary for CO.

| Vehicle type | R-square (%) | R-square (adj) (%) | R-square (pred) (%) |
|---|---|---|---|
| Petrol | 99.89 | 99.84 | 99.76 |
| Diesel | 85.91 | 83.9 | 76.15 |

be asserted that the formulated regression models are a dependable approach for accurately predicting CO emission from both petrol and diesel vehicles.

### 3.3. General factorial regression for HC

Figs. 13 and 14 depict the HC emissions for various road gradients in petrol and diesel vehicles, respectively. Lower HC emissions were observed at 30 km/h for both types of vehicles. For petrol vehicles, the HC emissions exhibited a decreasing trend as the road slope increased from a level surface to 4-degree angles, with peak HC noted at a 6-degree road slope. Conversely, for diesel vehicles, an increase in HC emissions rate was observed as the road slope increased from −2 to 4-degree, followed by a decrease as the slope increased further. The decline in HC emissions for petrol vehicles at, higher angles may be attributed to increased engine load, which reduces HC emissions (Xing et al., 2017). On the contrary, for diesel vehicles, the initial rise in HC emissions rate at a lower angle is likely due to reduced engine load (Liu et al., 2018), preventing the engine from reaching its optimal combustion temperature, and resulting in incomplete combustion and increased HC emissions (Wu et al., 2019).

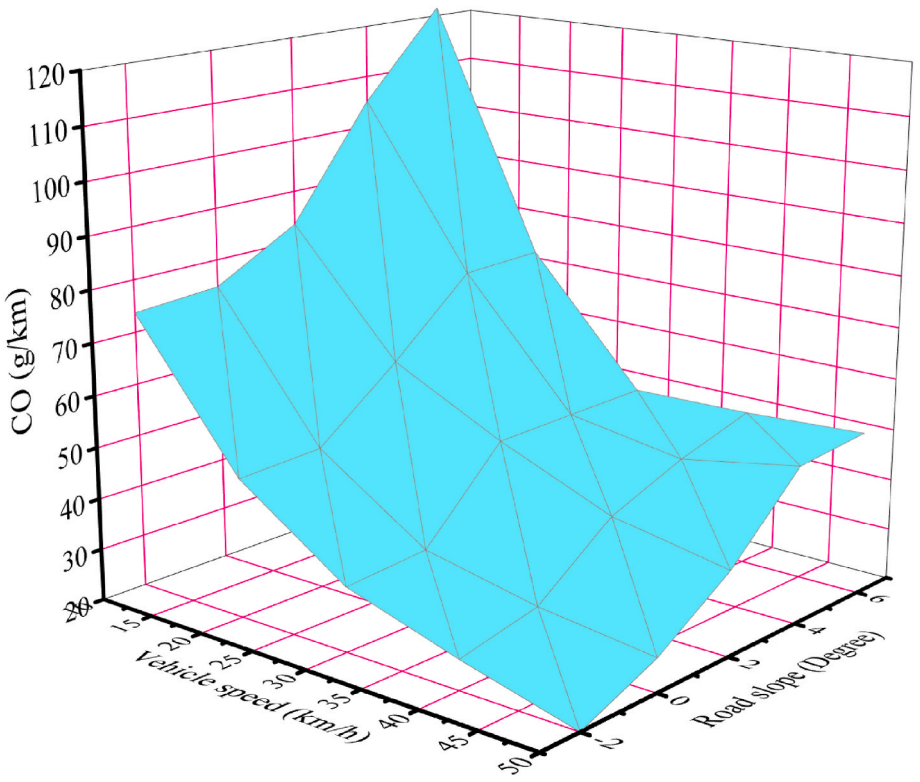


**Fig. 11.** Surface plot of CO emissions of petrol vehicles.

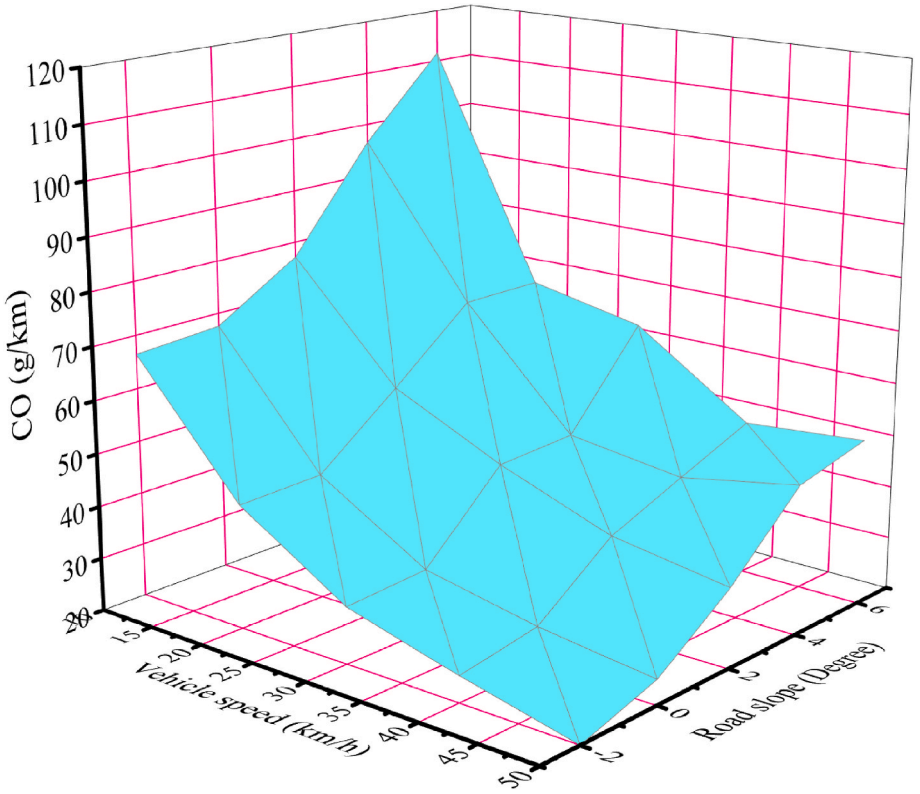


**Fig. 12.** Surface plot of CO emissions of diesel vehicles.

On a level road, the HC emissions rates for petrol vehicles on roads with slopes of −2°, 2°, and 4° did not significantly differ. However, uphill driving at a 6-degree angle led to a 27% increase in HC emissions. Similarly, for diesel vehicles the HC emissions rate on roads with slopes of −2 and 2° did not significantly differ from the level road, while on 4° and 6° uphill routes, HC increased by 20.83% and 13.44%, respectively.

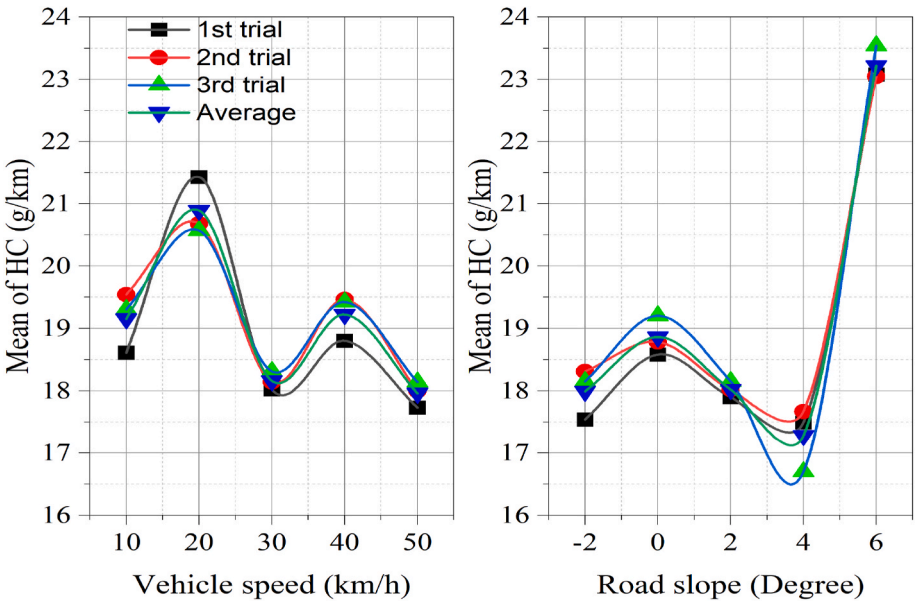


**Fig. 13.** HC main effect plot for petrol vehicle.

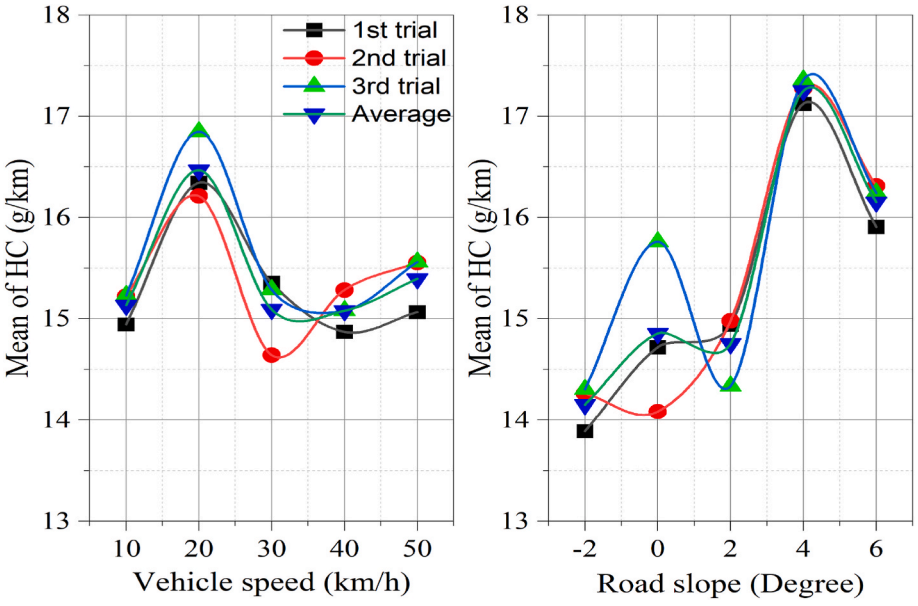


**Fig. 14.** HC main effect plot for diesel vehicle.

Results from this study indicate that diesel vehicles emitted 20.98%, 21.18%, 16.89%, 21.55%, and 14.29% lower HC emissions than petrol vehicles at speeds of 10, 20, 30, 40, and 50 km/h. Additionally, the HC emissions from petrol vehicles at −2, 0, 2, 4, and 6 degrees of road gradient were 21.33%, 21.24%, 18.13%, 0.16%, and 30.44% higher than those of diesel vehicles, respectively.

The regression models fitted for HC emissions in petrol and diesel are presented in equations (11) and (12), respectively. The values of R-square and adjusted R-square, as indicated in Table 6, demonstrates that both regression models for petrol and diesel vehicles exhibited the highest levels of accuracy.

$$HC\ (g/km) = 19.09 + 0.0302 \times V + 0.598 \times S - 0.00052 \times V \times S \quad (11)$$

$$HC\ (g/km) = 14.647 + 0.0049 \times V + 0.523 \times S - 0.00676 \times V \times S \quad (12)$$

where V is vehicle velocity in km/h, and S is road slope in degree.

**Table 6**
Model summary for HC.

| Vehicle type | R-square (%) | R-square (adj) (%) | R-square (pred) (%) |
|---|---|---|---|
| Petrol | 96.65 | 95.04 | 92.46 |
| Diesel | 73.12 | 72.57 | 70.63 |

### 3.4. Desirability functionality analysis (DFA)

An assessment of the DFA was carried out for the chosen road slopes following the FFA. This DFA aimed to pinpoint optimal points that simultaneously minimize the formation of CO, HC, and $CO_2$ on pre-determined routes. Table 7 showcases the top three solutions obtained from experimental results during tests conducted on various road slopes and vehicle speeds for the selected vehicles under consideration.

**Table 7**
Solutions of DFA.

| Vehicle Speed (km/h) | Road Slope (deg) | Mean of HC (g/km) | Mean of CO (g/km) | Mean of $CO_2$ (g/km) | Composite Desirability |
|---|---|---|---|---|---|
| 40 | −2 | 15.445 | 23.549 | 117.892 | 0.948 |
| 50 | −2 | 15.973 | 17.734 | 118.134 | 0.948 |
| 30 | −2 | 15.497 | 16.518 | 128.587 | 0.948 |
| 40 | 0 | 16.753 | 19.999 | 153.677 | 0.831 |
| 30 | 0 | 16.225 | 25.815 | 153.436 | 0.827 |
| 50 | 0 | 16.276 | 18.784 | 164.13 | 0.821 |
| 30 | 2 | 15.757 | 33.765 | 191.143 | 0.72 |
| 40 | 2 | 16.285 | 31.55 | 191.224 | 0.709 |
| 50 | 2 | 15.808 | 30.334 | 201.678 | 0.694 |
| 40 | 4 | 17.165 | 42.283 | 220.085 | 0.556 |
| 30 | 4 | 16.638 | 48.098 | 219.844 | 0.555 |
| 50 | 4 | 16.689 | 41.067 | 230.538 | 0.528 |
| 30 | 6 | 19.055 | 54.492 | 257.58 | 0.285 |
| 40 | 6 | 19.583 | 48.676 | 257.821 | 0.281 |
| 20 | 6 | 21.111 | 69.268 | 252.954 | 0.243 |

According to Table 7 and Fig. 15 (A), at −2° slopes, speeds of 40 km/h, 50 km/h, and 30 km/h exhibit nearly identical composite desirability indexes of 0.948. This suggests that the composite desirability is not influenced by vehicle speed on the −2° road slope. Conversely, as Table 7 and Fig. 15 (B) show, the composite desirability indexes for speeds of 40 km/h, 30 km/h, and 50 km/h on level road were 0.831, 0.827, and 0.821, respectively. The highest composite desirability index was observed at 40 km/h, signifying that this speed is optimal for minimizing CO, HC, and $CO_2$ emissions on level roads. This speed allows vehicles to travel on the flat road at a moderate speed, promoting efficient fuel usage. Consequently, the simultaneous reduction of $CO_2$, CO, and HC emissions was achieved. Consequently, this concurrently lowers emissions of $CO_2$, CO, and HC. On 2-degree road slopes, the composite desirability indexes were 0.72, 0.709, and 0.694 for speeds of 30 km/h, 40 km/h, and 50 km/h, respectively. Notably, the most favourable speed for minimizing CO, HC, and $CO_2$ emissions on 2-degree road slopes is found 30 km/h, as shown in Fig. 15 (C). This discovery underscores the preference for a speed 30 km/h to achieve emission reduction on roads with a 2-degree slope, affirming the effectiveness of speed limits in mitigating environmental impact. In contrast, the best three composite desirability indexes for roads with 4° and 6-degree slopes were all below 0.7. In comparison to other road angles, the outcome lacks significance. Consequently, roads with 4° or 6° are deemed unsuitable for optimizing speed operations. Therefore, imposing vehicle speed limits on 4° and 6° road slopes may not contribute significantly to reduce emissions.

Generally, the utilization of DFA in this study demonstrated that, in comparison to the optimized speed of 40 km/h for vehicles, traveling at a speed of 30 km/h on a level road led to an increase of 2.82% in $CO_2$ emissions, 18.97% in CO emissions, and 5.28% in HC emissions. As per the findings, when the optimized vehicle speed of 30 km/h on a 2-degree road incline was compared, operating at a speed of 20 km/h on the 2-degree gradient resulted in a 4% rise in $CO_2$ emissions, a 23.92% reduction in CO emissions, and a 1.26% decline in HC emissions.

## 4. Conclusions

In internal combustion vehicles, efforts to minimize pollutant gases such as CO and HC often inadvertently lead to increased $CO_2$ levels. Simultaneously mitigating CO, HC, and $CO_2$ has not been thoroughly investigated. To address this, this study proposes a novel approach utilizing DFA to optimize vehicle speeds for urban roads with various slopes. This study used a portable emissions tester to experimentally assess the simultaneous reduction in vehicle tailpipe emissions using DFA across five diverse vehicle speeds and five distinct road slopes in Addis Ababa, Ethiopia. This assessment aimed to identify the optimal speed for minimizing $CO_2$, HC, and CO emissions simultaneously. Employing DFA, this study discovered the most effective combination of speed and slope that led to emission reduction. These findings hold potential for enhancing the sustainability of transportation by significantly lowering vehicle emissions. Based on the experimental findings, the following conclusions have been drawn.

For petrol vehicles, the $CO_2$ emissions on roads with road slopes of 2°, 4°, and 6° were 16.25%, 28.58%, and 43.36% higher, respectively, compared to level roads. In the case of diesel vehicles $CO_2$ emissions increased by 53.7%, 91.08%, and 245.85% on gradients of 2°, 4°, and 6° while, a 36% reduction was observed on −2° slope compared to a level road. CO emissions generally increased with steeper road slopes and decreases with higher vehicle speeds. Both petrol and diesel vehicles emitted lower levels of HC at a speed of 30 km/h. Moreover, the composite desirability index was highest at 40 km/h on a level road and 30 km/h on a 2° slope, representing the optimum speeds to simultaneously

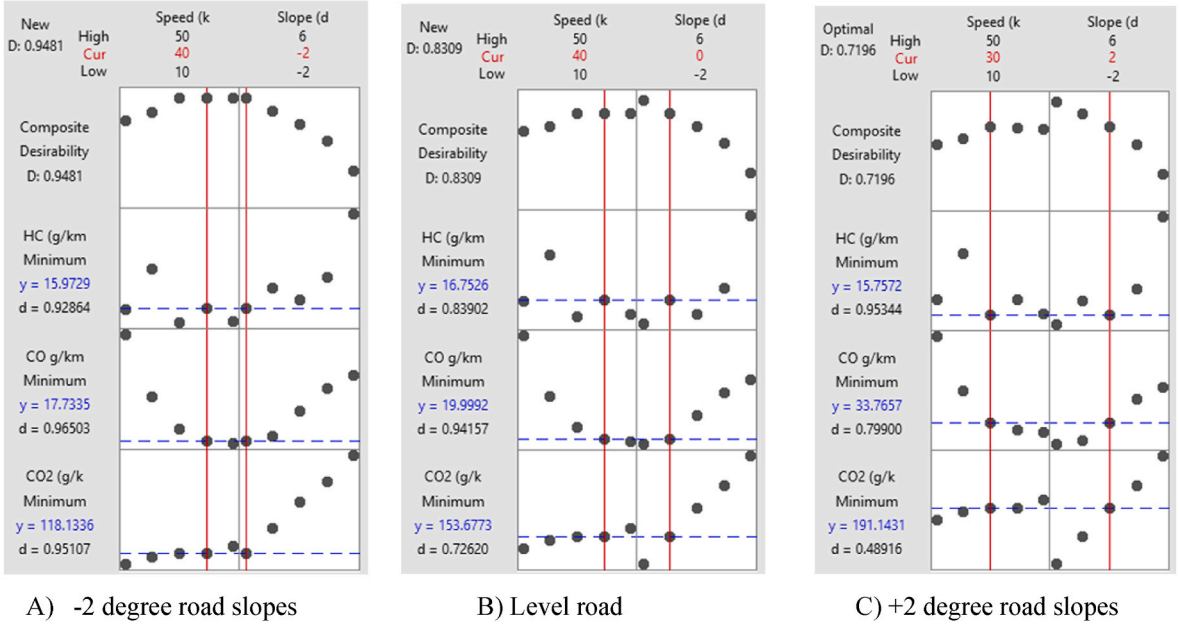


**Fig. 15.** Plots of the response optimization of DFA.

minimize CO, HC, and $CO_2$ emission. Notably, speed of 30 km/h, 40 km/h, and 50 km/h exhibited nearly equal composite desirability indexes of 0.948 on $-2^{\circ}$ road slopes. In light of these findings, it is recommended that urban speed limits consider both $CO_2$, HC, and CO emissions to achieve simultaneous minimization. This study revealed that, compared to the optimized vehicle speed of 40 km/h, emissions at a speed of 30 km/h on a flat road increased $CO_2$ by 2.82%, CO by 18.97%, and HC by 5.28%. According to this study, when compared to the optimized vehicle speed of 30 km/h on a 2-degree road gradient, a speed of 20 km/h on the same gradient resulted in a 4% increase in $CO_2$ emissions, a 23.92% increase in CO emissions, and a 1.26% decrease in HC emissions.

The obtained results offer a practical strategy for emission reduction in internal combustion engines, applicable across different engine types and vehicles. This study findings not only identified the optimal speed for minimizing $CO_2$, HC, and CO emissions simultaneously but also revealed an interaction between vehicle speed and road slope for effective emission reduction. These results have the potential to significantly enhance the sustainability of transportation by lowering vehicle emissions. The study also emphasizes the importance of considering composite desirability indexes for determining optimal speeds under various conditions. Furthermore, it recommends that urban speed limits shall consider $CO_2$, HC, and CO emissions collectively to achieve simultaneous minimization, providing valuable guidance for urban planning and the development of emission reduction strategies within the transportation sector. Furthermore, this study can serve as a valuable reference for future research aimed at reducing emissions within the transportation sector.

## Funding

This research was funded by Adama Science and Technology University (ASTU), Adama, Ethiopia for A.G.A.'s doctoral financial support.

## Institutional review board statement

Not applicable.

## Informed consent statement

Not applicable.

## CRediT authorship contribution statement

**Amanuel Gebisa:** Conceptualization, Data curation, Formal analysis, Investigation, Methodology, Software, Writing – original draft, Writing – review & editing. **Girma Gebresenbet:** Conceptualization, Methodology, Supervision, Validation, Visualization, Writing – review & editing. **Rajendiran Gopal:** Conceptualization, Formal analysis, Investigation, Methodology, Supervision, Writing – review & editing. **Ramesh Babu Nallamothu:** Conceptualization, Formal analysis, Investigation, Methodology, Supervision, Writing – review & editing.

## Declaration of competing interest

We confirm that this work is original and has not been published elsewhere, nor is it currently under consideration for publication elsewhere.

We believe that this manuscript is appropriate for publication by Cleaner Engineering and Technology because it aligns with the journal's Aims and scope.

We have no conflicts of interest to disclose.

## Data availability

Data will be made available on request.

## Acknowledgements

The authors express their gratitude to Yeron Ride Service PLC, Dr. Keredin Abatamam, Mr. Chali Petros, and Mulu Negawo for their assistance in gathering data. Additionally, appreciation is extended to the Swedish University of Agricultural Science for providing us with a portable emission analyzer.

## References

Alhassan Sati, S., Johnson Dare, A., 2022. An analysis of the level of vehicular emission in kaduna metropolis. Ghana Journal of Geography 14 (1). https://doi.org/10.4314/gjg.v14i1.1.

Ali, M., Sheha, A., Tsokos, C.P., Mamudu, L., 2022. Desirability function approach to response surface optimization analysis of atmospheric carbon dioxide CO2 emissions in Africa. Glob. J. Sci. Front. Res. (GJSFR) H 22 (7), 1–10.

Costagliola, M.A., Costabile, M., Prati, M.V., 2018. Impact of road grade on real driving emissions from two euro 5 diesel vehicles. Appl. Energy 231, 586–593. https://doi.org/10.1016/j.apenergy.2018.09.108.

Cvitanić, D., Breški, D., Maljković, B., 2023. Impact of road alignment on fuel consumption and gas emissions – experimental and analytical research. Advances in Civil and Architectural Engineering 14 (26), 40–53. https://doi.org/10.13167/2023.26.4.

Devarajaiah, D., Muthumari, C., 2018. Evaluation of power consumption and MRR in WEDM of Ti–6Al–4V alloy and its simultaneous optimization for sustainable production. J. Braz. Soc. Mech. Sci. Eng. 40 (8) https://doi.org/10.1007/s40430-018-1318-y.

Donateo, T., Filomena, R., 2020. Real time estimation of emissions in a diesel vehicle with neural networks. E3S Web of Conferences 197, 06020. https://doi.org/10.1051/e3sconf/202019706020.

Gallus, J., Kirchner, U., Vogt, R., Benter, T., 2017. Impact of driving style and road grade on gaseous exhaust emissions of passenger vehicles measured by a portable emission measurement system (PEMS). Transport. Res. Part D 52 (2), 215–226. https://doi.org/10.1016/j.trd.2017.03.011.

Karimipour, H., Tam, V.W.Y., Le, K.N., Burnie, H., 2021. Routing on-road heavy vehicles for alleviating greenhouse gas emissions. Cleaner Engineering and Technology 5, 100325. https://doi.org/10.1016/J.CLET.2021.100325.

Liu, H., Ma, J., Dong, F., Yang, Y., Liu, X., Ma, G., Zheng, Z., Yao, M., 2018. Experimental investigation of the effects of diesel fuel properties on combustion and emissions on a multi-cylinder heavy-duty diesel engine. Energy Convers. Manag. 171, 1787–1800. https://doi.org/10.1016/J.ENCONMAN.2018.06.089.

Liu, H., Rodgers, M.O., Guensler, R., 2019. Impact of road grade on vehicle speed-acceleration distribution, emissions and dispersion modeling on freeways. Transport. Res. Transport Environ. 69, 107–122. https://doi.org/10.1016/j.trd.2019.01.028.

Meena, S., Singh, S.K., 2022. Assessment of real driving emissions from vehicles using portable emission measurement systems: a systematic review. Appl. Ecol. Environ. Sci. 10 (5), 273–280. https://doi.org/10.12691/aees-10-5-2.

Meng, X., Pang, K., Di, B., Li, W., Wang, Y., Zhang, J., Xu, Y., 2023. Road grade estimation for vehicle emissions modeling using electronic atmospheric pressure sensors. Front. Environ. Sci. 10 https://doi.org/10.3389/fenvs.2022.1051858.

Pavlovic, J., Fontaras, G., Ktistakis, M., Anagnostopoulos, K., Komnos, D., Ciuffo, B., Clairotte, M., Valverde, V., 2020. Understanding the origins and variability of the fuel consumption gap: lessons learned from laboratory tests and a real-driving campaign. Environ. Sci. Eur. 32 (53), 1–16. https://doi.org/10.1186/s12302-020-00338-1.

Perec, A., 2022. Desirability function analysis (DFA) in multiple responses optimization of abrasive water jet cutting process. Reports in Mechanical Engineering 3 (1), 11–19. https://doi.org/10.31181/rme200103011p.

Pilusa, T.J., Mollagee, M.M., Muzenda, E., 2012. Reduction of vehicle exhaust emissions from diesel engines using the whale concept filter. Aerosol Air Qual. Res. 12 (5), 994–1006. https://doi.org/10.4209/aaqr.2012.04.0100.

Posada-Henao, J.J., Sarmiento-Ordosgoitia, I., Correa-Espinal, A.A., 2023. Effects of road slope and vehicle weight on truck fuel consumption. Sustainability 15 (1). https://doi.org/10.3390/su15010724.

Salihu, F., Demir, Y.K., Demir, H.G., 2023. Effect of road slope on driving cycle parameters of urban roads. Transport. Res. Transport Environ. 118, 103676 https://doi.org/10.1016/J.TRD.2023.103676.

Šarkan, B., Loman, M., Synák, F., Skrúcaný, T., Hanzl, J., 2022. Emissions production by exhaust gases of a road vehicle's starting depending on a road gradient. Sensors 22 (24). https://doi.org/10.3390/s22249896.

Shepelev, V., Glushkov, A., Slobodin, I., Cherkassov, Y., 2023. Measuring and modelling the concentration of vehicle-related PM2.5 and PM10 emissions based on neural networks. Mathematics 11 (5). https://doi.org/10.3390/math11051144.

Sher, F., Chen, S., Raza, A., Rasheed, T., Razmkhah, O., Rashid, T., Rafi-ul-Shan, P.M., Erten, B., 2021. Novel strategies to reduce engine emissions and improve energy efficiency in hybrid vehicles. Cleaner Engineering and Technology 2, 100074. https://doi.org/10.1016/J.CLET.2021.100074.

Thorisingam, Y., Mustafa, M.S., 2022. Augmented approach to desirability function based on principal component analysis. Int. J. Acad. Res. Prog. Educ. Dev. 11 (2) https://doi.org/10.6007/ijarped/v11-i2/13270.

Triantafyllopoulos, G., Dimaratos, A., Ntziachristos, L., Bernard, Y., Dornoff, J., Samaras, Z., 2019. A study on the CO2 and NOx emissions performance of euro 6 diesel vehicles under various chassis dynamometer and on-road conditions including

latest regulatory provisions. Sci. Total Environ. 666, 337–346. https://doi.org/10.1016/j.scitotenv.2019.02.144.

Wang, Y., Zhao, H., Yin, H., Yang, Z., Hao, L., Tan, J., Wang, X., Zhang, M., Li, J., Lyu, L., Wang, H., Wang, C., Tan, D., Ge, Y., 2022. Quantitative study of vehicle CO2 emission at various temperatures and road loads. Fuel 320, 123911. https://doi.org/10.1016/j.fuel.2022.123911.

Wu, Y., Wang, P., Muhammad Farhan, S., Yi, J., Lei, L., 2019. Effect of post-injection on combustion and exhaust emissions in DI diesel engine. Fuel 258, 116131. https://doi.org/10.1016/J.FUEL.2019.116131.

Xing, J., Shao, L., Zheng, R., Peng, J., Wang, W., Guo, Q., Wang, Y., Qin, Y., Shuai, S., Hu, M., 2017. Individual particles emitted from gasoline engines: impact of engine types, engine loads and fuel components. J. Clean. Prod. 149, 461–471. https://doi.org/10.1016/J.JCLEPRO.2017.02.056.